Gurley, L. R., Walters, R. A., & Tobey, R. A. (1975) *J. Biol. Chem. 250*, 3936.
Gurley, L. R., D'Anna, J. A., Barham, S. S., Deaven, L. L., & Tobey, R. A. (1978) *Eur. J. Biochem. 84*, 1.
Hohmann, P., Tobey, R. A., & Gurley, L. R. (1976) *J. Biol. Chem. 251*, 3685.
Johns, E. W. (1964) *Biochem. J. 92*, 55.
Kinkade, J. M., & Cole, R. D. (1966) *J. Biol. Chem. 241*, 5790.
Laemmli, U. K. (1970) *Nature (London) 227*, 680.
Panyim, S., & Chalkley, R. (1969a) *Biochem. Biophys. Res. Commun. 37*, 1042.
Panyim, S., & Chalkley, R. (1969b) *Biochemistry 8*, 3972.
Perhson, J., & Cole, R. D. (1980) *Nature (London) 285*, 43.
Pochron, S. F., & Baserga, R. (1979) *J. Biol. Chem. 254*, 6352.
Seyedin, S. M., & Kistler, W. S. (1979) *Biochemistry 18*, 1371.
Smerdon, M. J., & Isenberg, I. (1976) *Biochemistry 15*, 4233.
Smith, B. J., & Johns, E. W. (1980) *FEBS Lett. 110*, 25.
Smith, B. J., Walker, J. M., & Johns, E. W. (1980) *FEBS Lett. 112*, 42.
Spackman, D. H., Stein, W. H., & Moore, S. (1958) *Anal. Chem. 30*, 1190.
Tobey, R. A., Petersen, D. F., Anderson, E. C., & Puck, T. T. (1966) *Biophys. J. 6*, 567.

Phase Equilibria in Binary Mixtures of Phosphatidylcholine and Cholesterol†

Diether J. Recktenwald and Harden M. McConnell*

ABSTRACT: The paramagnetic resonance spectra of two spin-labels, 2,2,6,6-tetramethylpiperadinyl-1-oxy and a head-group spin-labeled phosphatidylethanolamine (L-α-dipalmitoylphosphatidyl-*N*-ethanolamine), have been used to study solid–liquid and liquid–liquid phase separations in binary mixtures of dimyristoylphosphatidylcholine and cholesterol. A quantitative analysis of these resonance spectra supports the view that at temperatures below θ_m, the chain-melting temperature of the phospholipid, and at cholesterol mole fractions $X_c < 0.2$, these mixtures consist of two phases, a solid phase of essentially pure dimyristoylphosphatidylcholine and a fluid phase having a mole fraction of cholesterol equal to 0.2. The spin-label data also provide evidence for fluid–fluid immiscibility in the bilayer membrane at temperatures above the chain-melting transition temperature of dimyristoylphosphatidylcholine.

There have been numerous studies of the physical properties of lipid bilayers containing binary mixtures of phosphatidylcholine and cholesterol. A number of early attempts to interpret these physical properties in terms of molecular structure and dynamics are flawed by failure to take into account the lateral phase separations in these mixtures. As discussed later, the cholesterol–phosphatidylcholine bilayer membrane does exhibit solid phase–fluid phase phase separations and also very probably fluid phase–fluid phase phase separations. Previous attempts to derive phase diagrams for these binary mixtures have been made by Shimshick & McConnell (1973a) and Lentz et al. (1980). In contrast to the numerous reported diagrams for mixtures of phospholipids [see, e.g., Shimshick & McConnell (1973b)], there is considerable uncertainty about many features of all of the proposed phase diagrams for binary mixtures containing cholesterol. However, in one limited temperature-composition region, the composition and some physical properties of the two coexisting phases have become clear, at least for binary mixtures of dipalmitoylphosphatidylcholine (DPPC)[1] [or dimyristoylphosphatidylcholine (DMPC)] and cholesterol (Copeland & McConnell, 1980; Owicki & McConnell, 1980; Rubenstein et al., 1979, 1980). At temperatures θ below the main chain-melting transition temperature, θ_m, of the phospholipid and for cholesterol mole fractions, X_c, less than approximately 0.2, the two coexisting phases are "solid" and "fluid". The solid phase is essentially pure DMPC (or DPPC), and the fluid phase contains ~20 mol % cholesterol. We use the terms solid and fluid for lipid phases where lipid lateral diffusion coefficients are small (10^{-10}–10^{-11} cm^2/s, characteristic of gel phase lipids, or large (10^{-9}–10^{-7} cm^2/s), characteristic of lipid mixtures at temperatures above the θ_m for all the phospholipids. This temperature-composition region is denoted by II in Figure 1. The binary mixtures in region II have a remarkable domain structure consisting of (approximately) parallel domains of solid and fluid lipid as judged by freeze–fraction electron microscopy (Copeland & McConnell, 1980). With increasing cholesterol concentration, the widths of the parallel solid domains remain nearly constant and equal to one another while their separation increases, in proportion to the increase of fluid lipid. Our earlier conclusions regarding the coexisting phases in region II are based primarily on freeze–fracture electron microscopy (Copeland & McConnell, 1980), studies of lateral diffusion of fluorescent lipid probes (Rubenstein et al., 1979; Owicki & McConnell, 1980), and scanning calorimetry (Mabrey et al., 1978). Additional discussion of the lipid bilayer structure in region II can be found in Rubenstein et al. (1980). Quite recent studies of rotational diffusion of a fluorescent lipid probe also support the above conclusions regarding the coexisting phases in region II (Smith et al., 1981).

† From the Department of Chemistry, Stanford University, Stanford, California 94305. *Received December 30, 1980.* This work has been supported by National Science Foundation Grant PCM 77-23586, by The Alexander Medical Foundation, and by Research Fellowship Re 493/1 to D.J.R. from the Deutsche Forschungsgemeinschaft.

[1] Abbreviations used: DMPC, dimyristoylphosphatidylcholine; DPPC, dipalmitoylphosphatidylcholine; EPR, electron paramagnetic resonance; Tempo, 2,2,6,6-tetramethylpiperidinyl-1-oxy; PBS, phosphate-buffered saline.

0006-2960/81/0420-4505$01.25/0

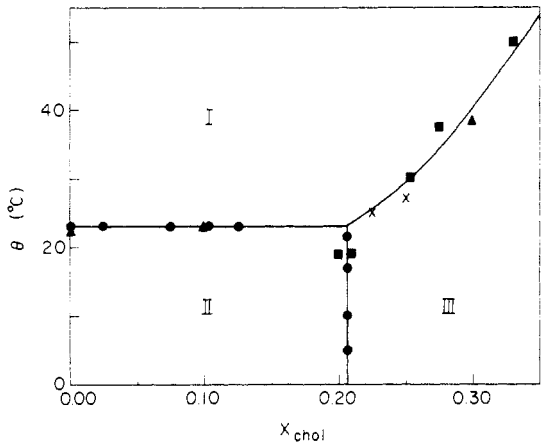

FIGURE 1: Phase diagram for DMPC–cholesterol as obtained from EPR methods. Tempo partitioning: (▲) temperature scan; (■) composition variation. Spin-label I spectra: (●) normalized spectral line height; (×) hyperfine splitting.

The above description of the coexisting phases in region II is quite extraordinary: for example, we know of no other physical system exhibiting regularly alternating fluid and solid domains. Since molecular explanation of this apparently unique membrane structure is not known as yet, it is clearly appropriate to test every facet of our description of the structure so as to ensure its accuracy. The present spin-label study was undertaken primarily to test our previous descriptions of the stoichiometries of the two coexisting phases in region II. Our data also provide evidence in favor of coexisting but immiscible fluid membrane in region I. From the latter result, one can readily extrapolate to the probable coexistance of immiscible fluid regions in biological membranes.

Materials and Methods

Dimyristoylphosphatidylcholine was obtained from Sigma (St. Louis, MO). Cholesterol from Reheis Chemical Co. (Phoenix, AZ) was recrystallized twice from ethanol. Separately synthesized samples of spin-label I were gifts of Drs. P. Brûlet and M. McCloskey. The synthesis of I is described by Kornberg & McConnell (1971). Liposomes were prepared as described by Rubenstein et al. (1980). For the measurement of Tempo partitioning, a dry phospholipid film containing a total of 10 μmol of phospholipid and cholesterol was hydrated above the DMPC phase-transition temperature with 1 mL of phosphate-buffered saline (PBS) containing 1.0×10^{-4} M Tempo. After 10-s vortexing, the sample was spun down at 100*g* for 2 min. The supernatant was removed so as not to disturb the liposome pellet. The liposomes were washed once with Tempo-PBS at the temperature of the measurements to maintain a constant solution concentration of Tempo. The last pellet was resuspended in 50 μL of additional PBS, 1.0×10^{-4} M in Tempo, by gentle vortexing and then transferred into a 100-μL capillary tube containing a small piece of glass to allow efficient mixing of the liposome suspension. EPR spectra were taken as described in Rubenstein et al. (1980). Our experimental paramagnetic spectra are discussed in terms of spectral normalized line heights (L), which refer to signal amplitudes for a constant spectral area, i.e., constant spin concentration.

Results

Tempo partitioning into phospholipid–cholesterol liposomes was measured by monitoring the resolved high-field EPR signals for hydrocarbon- and water-dissolved spin-label. As shown in Figure 2a, partitioning ratios β' measured below the phospholipid phase transition at 19 °C decrease linearly from

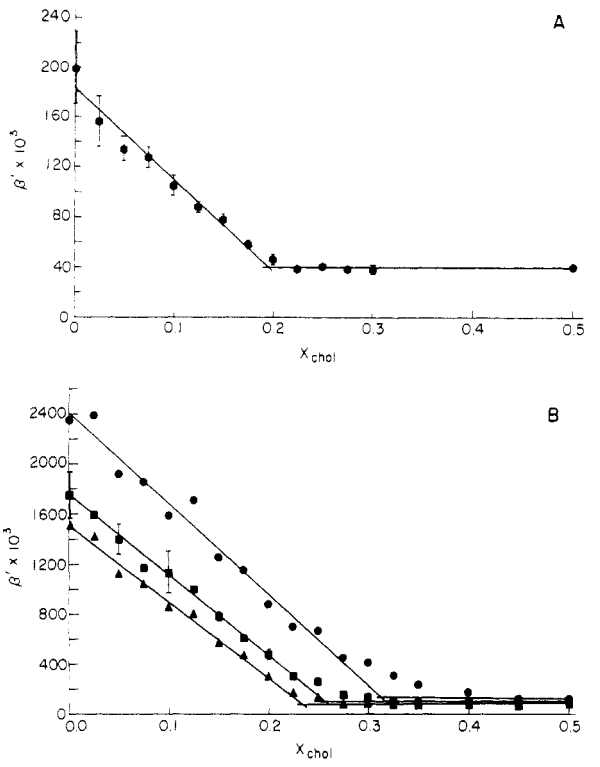

FIGURE 2: Tempo partitioning into DMPC–cholesterol liposomes from a 1×10^{-4} M solution at (A) 20, (B) (▲) 30, (■) 37, and (●) 50 °C (β' is defined in Appendix Ia).

0.18 to 0.04 as the liposomes' cholesterol content increases in the 0–20% range. Here β' is the EPR peak amplitude in the hydrocarbon phase divided by the EPR peak amplitude in the aqueous phase. Between 20% and 50% cholesterol, the shape of the curve cannot be further resolved because with a partition ratio of 0.04 Tempo is almost insoluble in these liposomes. Above the DMPC phase-transition temperature, qualitatively the same behavior is observed as described above, as shown in Figure 2B. The breakpoint, however, is shifted to higher cholesterol concentrations, i.e., 24% at 30 °C, 26% at 37 °C, and 32% at 50 °C. As will be discussed below, these observations indicate a two-phase region at low cholesterol concentrations both below and above the phospholipid main phase-transition temperature.

In an effort to characterize further the binary DMPC–cholesterol system with respect to its dynamic properties and to confirm our conclusions by still another approach, the phospholipid spin-label I was used as a probe in liposomes.

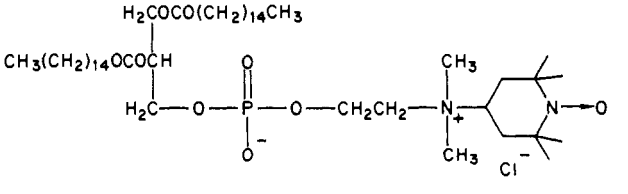

I

The influence of the cholesterol content of DMPC liposomes between 0% and 30% on the normalized line height $L1_N$ of the low-field line of the EPR spectrum of spin-label I in the temperature range between 5 and 50 °C was measured (at 1% probe concentration) (Figure 3). Between 5 and 22 °C (below the DMPC phase-transition temperature at about 23 °C), there is no significant change of the normalized line height at cholesterol concentrations below 10% cholesterol. Between 10% and 20% cholesterol, there is a monotonic increase in line height followed by a pronounced break to a smaller slope above 20% cholesterol.

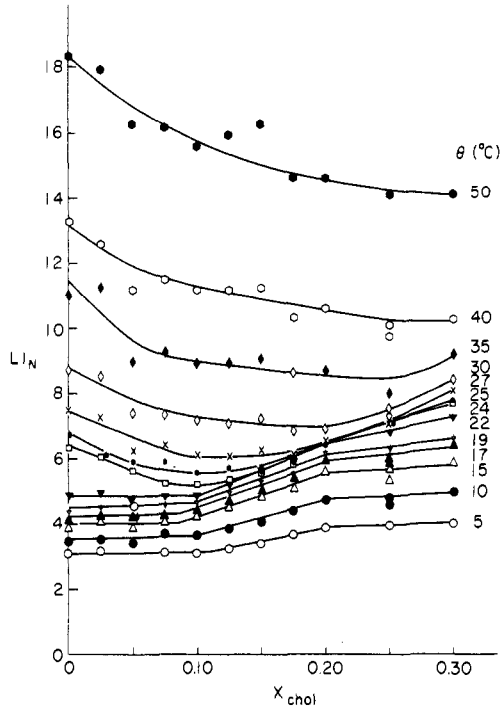

FIGURE 3: Normalized heights of the low-field line in the ESR spectrum of spin-label I in DMPC–cholesterol liposomes as a function of cholesterol content and temperature (spin-label concentration 1 mol %).

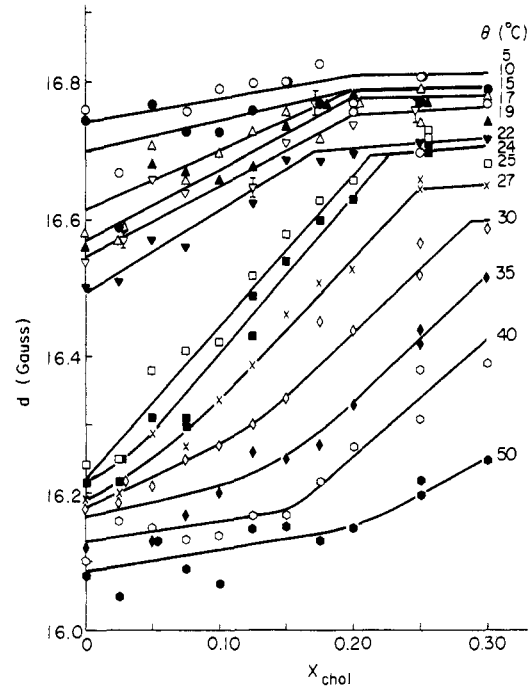

FIGURE 4: Hyperfine splitting d in the EPR spectrum of spin-label I in DMPC–cholesterol liposomes as a function of cholesterol content and temperature. (○) 5, (●) 10, (△) 15, (▲) 17, (▽) 19, (▼) 22, (□) 24, (■) 25, (×) 27, (◇) 30, (◆) 35, (□) 40, and (◆) 50 °C (spin label concentration 1 mol %).

Above 23 °C, there is a significant decrease in line height with increasing cholesterol concentrations followed by an increase. For measurements performed above 23 °C, the minimum in line height moves to higher cholesterol concentrations with increasing temperature. In temperature scans through the phase-transition temperature, a significant jump in line height is only observed below a cholesterol content of 10% in the liposomes.

The hyperfine splitting of the spin-label signal the DMPC–cholesterol liposomes changes by only 3% with respect to the extreme values under all temperature and concentration conditions used. The reproducibility of our hyperfine splitting measurements is about 0.3% (0.6% at lower temperaures). Nevertheless, the following observations should be noted from these data. Below the DMPC phase-transition temperature and at less than 20% cholesterol, there is a monotonic increase of the hyperfine splitting constant of the probe with the cholesterol concentration followed by an almost constant value at higher cholesterol concentrations. The same pattern is observed at temperatures above the phospholipid phase-transition temperature with the breakpoint, originally at 20% cholesterol, shifted to higher concentrations with increasing temperature. At 22 and 24 °C, below and above θ_m for DMPC, and up to 20% cholesterol, plots of the probe's hyperfine splitting constans vs. the cholesterol content in liposomes are linear, reaching a constant value above 20% cholesterol (Figure 4). The change in hyperfine splitting between 24 and 22 °C (d_{24}–d_{22}) is a linear function of cholesterol concentration up to 20%, also coming to a constant value above that concentration.

The effect of probe concentration on its spectra in liposomes was studied to account for the possible effect of probe partitioning between phases. For probe concentrations between 0.02% and 2%, a linear relationship of one over the square root of the normalized line height vs. the probe concentration was found, i.e., a linear relationship between line width and probe concentration. This is the expected result if there is no change

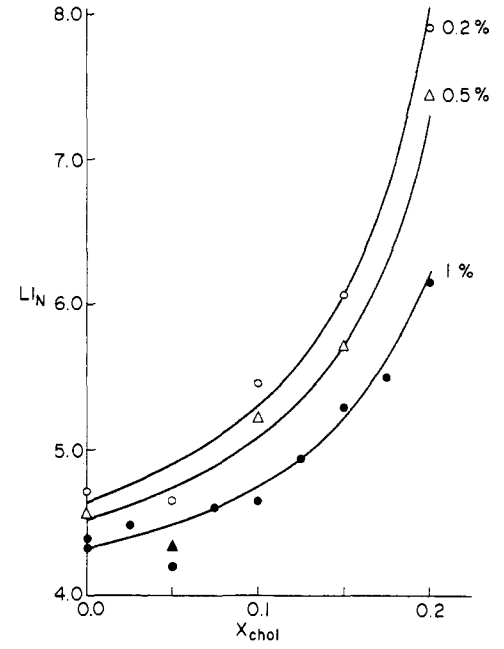

FIGURE 5: Calculated (lines) vs. measured values (points) of the normalized line height of the low-field line of the EPR spectrum of spin-label I in DMPC–cholesterol liposomes at 20 °C (a_1 = 2.1, b_1 = 0.46, a_2 = 6.1, b_2 = 0.34, and β = 4.38; see Appendix Ib).

in line shape with changes in probe concentration. Liposomes poor in cholesterol showed almost no decrease in normalized line heights with increasing probe concentrations whereas liposome containing cholesterol in excess of 20% showed a steep decrease in line height in these measurements.

Assuming a two-phase system, a calculation (see Appendix I) of line heights vs. cholesterol content was performed with the above data, using a linear combination of normalized line heights from the two pure phases. These pure phase were assumed to exist at 0% and 20% cholesterol below 23 °C and at about 25% cholesterol at 25 °C. The data in Figure 5 show

Table I: Normalized Spectral Line Heights[a] $L1_N$, $L2_N$, and $L3_N$ Extrapolated to Zero Concentration of Spin-Label I

temp (°C)	0% cholesterol			20% cholesterol			25% cholesterol		
	$L1_N$	$L2_N$	$L3_N$	$L1_N$	$L2_N$	$L3_N$	$L1_N$	$L2_N$	$L3_N$
20	4.5	5.7	0.89	8.6	10.5	2.3	10.4	11.9	2.8
25	6.3	5.9	0.87	8.2	9.0	2.2	11.1	12.8	3.3
50	22.7	16.0	4.3				18.9	14.8	4.0

[a] $L1_N$, $L2_N$, and $L3_N$ refer to the low-, middle-, and high-field components of the paramagnetic resonance hyperfine triplet of spin-label I.

that with an approximate 4-fold preference of the probe for the cholesterol-free phase at 19 °C, good agreement between calculated and experimental data is obtained at four different probe concentrations. In the same way, the region above 25 °C can be described in terms of a two-phase system. Table I shows the line heights at zero spin-label concentrations at 20, 25, and 50 °C in the pure phases. These numbers contain qualitative information about the dynamics of the probe in the various pure phases.

For the present study of phase equilibria using spin-labels, Tempo is superior to the phospholipid spin-label. This is because the Tempo partitioning between the lipid and the aqueous phase is easily measured and is a thermodynamic property of the system. The phospholipid spin-label would also be a powerful probe for the study of the phase equilibria if the resonance spectra of the probe were markedly different in the two phases (which they are not) and if the spin–spin interaction between labels could be neglected (which is not possible in our work). Nonetheless, the phospholipid spin-label data are important since they are in accord with our analysis of phase equilibria.

Discussion

The linear dependence of Tempo partitioning on the cholesterol content in DMPC liposomes at low cholesterol content strongly suggests two-phase systems both below and above the phospholipid gel to liquid-crystalline phase-transition temperature (23 °C). (See Appendix Ia.) The partition ratio β' which is measured in these experiments is directly proportional to the equilibrium constant of the process $(\text{Tempo})_{H_2O} \rightleftharpoons$ (Tempo) phospholipid. The sharp break observed at higher concentrations is due to a phase boundary which occurs at about 20% below 23 °C and moves to higher temperatures at higher cholesterol concentrations. Similar conclusions can be drawn from the EPR spectra of the phospholipid spin-label I in DMPC–cholesterol liposomes. Normalized line heights at different label and cholesterol concentrations can be adequately described by a linear combination of the line heights taking into account the partitioning between the two hydrophobic phases (Appendix Ib). Small deviations of the calculated from the experimental values are expected, because the calculation does not take into account the small change of hyperfine splitting with change in cholesterol content. As Figure 4 shows, this error is expected to be larger for values above 23 °C than below this temperature.

From the normalized line heights, the following conclusions can be drawn about the dynamic properties of the pure phases: Below 23 °C, addition of cholesterol increases the rotational mobility of the probe, as is evident from the rotational mobility in the 20% cholesterol-containing phase. This rotational mobility is indicated by the resonance lines narrowing and increases with increasing temperature.

Our interpretation of the resonance spectra for spin-label I shows how difficult it can sometimes be to locate phase boundaries from maxima or minima in spectroscopic parameters when competing effects are simultaneously present, such as the relative distribution of the label between two phases and line broadening due to probe–probe interactions. It is possible that this problem also is present in the case where fluorescence probes are used in the attempt to determine phase boundaries (Lentz et al., 1980). The interpretation of the spectroscopic data is clearly much simpler when they are directly related to the thermodynamic properties of the system, as in the case for Tempo partitioning.

We consider the spin-label data to be in excellent accord with the model of this two-phase region, described in the introduction. The phase boundary separting regions II and III has been established from spin-label data [Shimshick & McConnell (1973a) and the present work], calorimetric data (Mabrey et al., 1978), lipid diffusion data (Rubenstein et al., 1980; Owicki & McConnell, 1980) dilatometric data (Melchior et al., 1980), and the abrupt break in the lateral diffusion coefficients of a fluorescein-labeled protein incorporated in these lipid mixtures (Smith et al., 1980). The abrupt enhancement in diffusion of the fluorescent probes at 20 mol % has been attributed to the disappearance of the solid domains that act as barriers to lateral diffusion (Owicki & McConnell, 1980). An alternative interpreation of this abrupt enhancement in the rate of lateral diffusion has been given by Snyder & Freire (1980). These authors have suggested that the enhanced diffusion at approximately 20 mol % cholesterol is due to a "percolation effect", related to the statistical joining together of randomly distributed fluid zones so as to form long paths for diffusion. This model is at variance with our spin-label data (cf. Figure 2) since they picture the proportion of fluid lipid to still increase significantly after $X_c \approx 0.20$ whereas our data indicate the system to have a phase boundary at $X_c \approx 0.20$ (below θ_m).

Regions I and III are fluid in the sense that the lateral diffusion coefficients of fluorescent lipid probes are large. For example, when methods and materials similar to those described previously are used (Rubenstein et al., 1979), the diffusion coefficients of a fluorescent lipid probe in DMPC–cholesterol multilayers with $X_c = 0.30$ range from 2×10^{-9} cm^2/s at $\theta = 9.5$ °C to 1.1×10^{-7} cm^2/s at 50 °C (R. Weis, L. Smith, and H. McConnell, unpublished results). These phases (or mixtures of phases) are then, by definition, "fluid". It is interesting to note that not only are the boundaries between regions I and II and II and III detectable by abrupt changes in the diffusion coefficients of fluorescent lipid probes but also breaks in the temperature coefficients of probe lipid diffusion fall on the boundary separating regions I and II (R. Weis, L. Smith, and H. McConnell, unpublished results).

Note that according to the rules of construction of phase diagrams the boundaries of two-phase regions must meet at such angles that the extension of these boundaries (beyond the point of intersection) project into two-phase regions (Rhines, 1956). In the phase diagram, the boundary between I and III extends into II, two-phase region. Similarly, the boundary between II and III extends into I, also a two-phase region. There is a technical point concerning the number of phases in region II, and this is discussed in Appendix II.

Presumably, as the temperature is increased, a line is crossed where the two-phase region I is converted into a one-phase region. Shimshick & McConnell (1973a) proposed an upper boundary for the two-phase region I, but our present experiments (where both the data and data analysis have been improved over the earlier work) do not permit us to locate the upper boundary of region II. In this connection it should be

noted that Lentz et al. (1980) have proposed a phase diagram for DPPC–cholesterol mixtures that is far more complex than the obviously incomplete diagram given in Figure 1. Suffice it to say that the two-phase diagrams do have some phase boundaries in common. In the present study, we have not attempted to set out boundaries for the $P_{\beta'}$ phase, partly for reasons that will be clear from the discussion in Appendix II and partly because the nearly vertical boundary between regions II and III extends to temperatures well below those of the $P_{\beta'} \leftrightarrow L_{\beta'}$ phase transition of the pure phospholipid. We base this conclusion on the fact that the abrupt enhancement in lateral diffusion at $X_c \approx 0.2$ occurs at low temperatures where the characteristic $P_{\beta'}$ bands are absent (Rubenstein et al., 1979), so even under these conditions the alternating solid–fluid character of region II is retained.

The coexistence of immiscible fluid phases is of obvious biological signficiance since such coexisting phases should give rise to a preferential lateral and probably also transverse partitioning of membrane components. Moreover, it is well-known that in mammalian cells the plasma membrane and the membrane of subcellular organelles have different lipid compositions. It has never been clear how these membranes, all doubtless "fluid", could be thermodynamically stable in the presence of one another. The present work shows that fluid lipid (immiscible) membranes can be thermodynamically stable in the presence of one another.

Acknowledgments

We are indebted to Professor Charles Kittel for bringing infinitely adaptive crystal structures to our attention.

Appendix

(I) Relation of Spin-Label Spectra to Phase Boundaries Describing Lateral Phase Separations. (a) Tempo Partitioning. Consider first the data on the partitioning of Tempo between the aqueous phase and the hydrocarbon phase, appropriate to region II of the phase diagram. When there are two lipid phases, such as that there are N_1 moles of lipid (of both kinds) in phase 1 and N_2 moles of lipid (of both kinds) in phase 2, then the partition coefficient β' can be broken down into two components.

$$\beta' = (\beta_1 N_1 + \beta_2 N_2)/(N_1 + N_2) \quad (1)$$

$$= X_1\beta_1 + X_2\beta_2 \quad (2)$$

These equations hold for the case where the total number of moles (N) is kept constant, $N = N_1 + N_2$, β_1 is the partition coefficient for Tempo between N moles of phase 1 and water, and β_2 is the partition coefficient for Tempo between N moles of phase 2 and water. X_1 and X_2 are the mole fractions of all lipids in phases 1 and 2. If we let x_1, x_2, and x be the mole fraction of all molecules in phase 1 that are cholesterol, x_2 the mole fraction of all molecules in phase 2 that are cholesterol, and x the mole fraction of all molecules in the sample that are cholesterol, then it follows from the lever rule that

$$X_1 = (x_2 - x)/(x_2 - x_1) \quad (3)$$

For region II, $x_2 = 0.20$, $x_1 = 0$, and thus

$$\beta' = \beta_1(1 - 5x) + \beta_2(5x) \quad (4)$$

From this it is clear that the partition coefficient β' is a linear function of x, the mole fraction of cholesterol in the two-phase region, II, as seen in Figure 2A. Similar conclusions apply to the data in Figure 2B for region I of the phase diagram except that x_2 at the I–III phase boundary is greater than 0.20 and is temperature dependent.

(b) Phospholipid Spin-Label Partitioning. The solubility of the phospholipid spin-label I in water is totally negligible, and in region II of the phase diagram only the distribution of this spin-label between phase 1 and phase 2 need be considered. The known diffusion coefficients of spin-label lipids are sufficiently low that there is no significant averaging of the reasonance signals, so the total signal is simply the superposition of the signal label I in phase 1 and label I in phase 2. For a constant number n of moles of phospholipid spin-label, with $n \ll N$, and with n_1 moles of label in phases 1 and n_2 moles of label in phase 2, we may define a partition coefficient β where

$$\beta = (n_1/N_1)/(n_2/N_2) \quad (5)$$

From eq 5 one can easily show that

$$f_2 = X_2/[\beta + (1 - \beta)X_2] \quad (6)$$

Here f_2 is the fraction of the spin-label in phase 2 and X_2 and X_1 are obtained from eq 3. We have found experimentally that the normalized line heights for each phase (line heights at constant spectral area, i.e., constant spin concentration) vary with the concentration of spin-label (e.g., $f_1 n/X_1 N$) according to

$$L_N = 1/[af_1 n/(X_1 N) + b]^2 \quad (7)$$

For a given resonance line shape (i.e., Lorentzian), this is the relationship expected between line height and label concentration when spin–spin interactions increase line widths and decrease line heights. Note that because we are dealing with two phases and three distinct hyperfine lines, there are six equations of the form of eq 7. The values selected for a and b then depend on both the phase and hyperfine line. When two phases are present, the height for any given hyperfine line is calculated from

$$L_N = f_1/[a_1 f_1 n/(X_1 N) + b_1]^2 + f_2/[a_2 f_2 n/(X_2 N) + b_2]^2 \quad (8)$$

Note that from eq 3, 6, and 8, it is clear that L_N is not a simple linear function of x, the mole fraction of cholesterol in the sample. Calculated and observed normalized line heights are given in Figure 5 for various spin-label concentrations.

(II) Number of Thermodynamic Phases in Region II. Throughout this paper we have discussed region II in Figure 1 as though two distinct thermodynamic phases were present, a "solid" (small diffusion coefficient) and a "fluid", containig ~20 mol % cholesterol. Although we have no reason to doubt the validity of this physical picture, the remarkably regular lateral parallel ordering of the fluid and solid domains (especially at the lower cholesterol concentrations) does raise the question as to whether or not this system should be regarded as a single phase (i.e., regular structures with large unit cells) at each and every composition. For a discussion of a related problem, see the work by Anderson (1973) on "infinitely adaptive structures". We shall not attempt a thermodynamic treatment of such systems. What is important for us is that, as the periodicity becomes larger and larger (as $X_c \rightarrow 0.20$), one expects that at finite temperatures (but well below θ_m = 22 °C) the ordered phase will "melt", that is, the regular ordering of the parallel solid phase bands will disappear. This is observed experimentally. That is, below the chain melting transition temperature, the regularity of this domain ordering becomes weaker as $X_c \rightarrow 0.20$, but two clearly identifiable phases remain. Thus, in Figure 1 the extension of the I–III boundary does enter a two-phase region, region II, and the extension of the II–III boundary does enter the two-phase region I. Note also that according to the phase rule, if II were

a one-phase region, III would be a two-phase region. Then the I–III boundary would extend into a one-phase region (I), and this violates the above cited rule for the construction of phase diagrams for binary mixtures.

References

Anderson, J. S. (1973) *J. Chem. Soc., Dalton Trans.*, 1107–1115.

Copeland, B. R., & McConnell, H. M. (1980) *Biochim. Biophys. Acta 599*, 95–109.

Kornberg, R. D., & McConnell, H. M. (1971) *Biochemistry 10*, 1111–1120.

Lentz, B. R., Barrow, D. A., & Hoechli, M. (1980) *Biochemistry 19*, 1943–1954.

Mabrey, S., Mateo, P. L., & Sturtevant, J. M. (1978) *Biochemistry 17*, 2464–2468.

Melchior, D. L., Scavitto, F., & Steim, J. M. (1980) *Biochemistry 19*, 4828–4834.

Owicki, J. C., & McConnell, H. M. (1980) *Biophys. J. 30*, 383–397.

Rhines, F. N. (1956) in *Phase Diagrams in Metallurgy*, p 36, McGraw-Hill, New York.

Rubenstein, J. L. R., Smith, B. A., & McConnell, H. M. (1979) *Proc. Natl. Acad. Sci. U.S.A. 76*, 15–18.

Rubenstein, J. L. R., Owicki, J. C., & McConnell, H. M. (1980) *Biochemistry 19*, 569–573.

Shimshick, E. J., & McConnell, H. M. (1973a) *Biochem. Biophys. Res. Commun. 53*, 446–451.

Shimshick, E. J., & McConnell, H. M. (1973b) *Biochemistry 12*, 2351–2360.

Smith, L. M., Rubenstein, J. L. R., Parce, J. W., & McConnell, H. M. (1980) *Biochemistry 19*, 5907–5911.

Smith, L. M., Weis, R. M., & McConnell, H. M. (1981) *Biophys. J.* (in press).

Snyder, B., & Freire, E. (1980) *Proc. Natl. Acad. Sci. U.S.A. 77*, 4055–4059.